THE JOURNAL OF BIOLOGICAL CHEMISTRY
Vol. 280, No. 24, Issue of June 17, pp. 23397–23407, 2005
Printed in U.S.A.
© 2005 by The American Society for Biochemistry and Molecular Biology, Inc.

RecQ Family Members Combine Strand Pairing and Unwinding Activities to Catalyze Strand Exchange*

Received for publication, December 16, 2004, and in revised form, April 7, 2005
Published, JBC Papers in Press, April 20, 2005, DOI 10.1074/jbc.M414130200

Amrita Machwe‡, Liren Xiao‡, Joanna Groden§, Steven W. Matson¶, and David K. Orren‡‖

From the ‡Graduate Center for Toxicology, University of Kentucky, Lexington, Kentucky 40536-0305, the §Department of Molecular Genetics, Biochemistry, and Microbiology, University of Cincinnati College of Medicine, Cincinnati, Ohio 45267, and the ¶Department of Biology, University of North Carolina, Chapel Hill, North Carolina 27599

RecQ helicases are critical for maintaining genomic integrity. In this study, we show that three RecQ members (WRN, deficient in the Werner syndrome; BLM, deficient in the Bloom syndrome; and *Drosophila melanogaster* RecQ5b (dmRecQ5b)) possess a novel strand pairing activity. Furthermore, each of these enzymes combines this strand pairing activity with its inherent DNA unwinding capability to perform coordinated strand exchange. In this regard, WRN and BLM are considerably more efficient than dmRecQ5b, apparently because dmRecQ5b lacks conserved sequences C-terminal to the helicase domain that contribute to DNA binding, strand pairing, and strand exchange. Based on our findings, we postulate that certain RecQ helicases are structurally designed to accomplish strand exchange on complex replication and recombination intermediates. This is highly consistent with proposed roles for RecQ members in DNA metabolism and the illegitimate recombination and cancer-prone phenotypes associated with RecQ defects.

RecQ family members are 3′ to 5′ DNA helicases that function in genome maintenance. Prokaryotes and lower eukaryotes have one RecQ helicase, whereas humans have five (RECQ1, BLM, WRN, RECQ4, and RECQ5). Notably, Bloom, Werner, and Rothmund-Thomson syndromes are autosomal recessive diseases caused by loss of function of BLM, WRN, and RECQ4, respectively (1–3). Cancer incidence is markedly elevated in these syndromes (particularly in Bloom syndrome), although each has a distinct clinical phenotype. Werner syndrome is especially notable for the accelerated development of certain aging characteristics, including graying and loss of hair, atherosclerosis, cataracts, diabetes, and osteoporosis (4, 5). Thus, these diseases serve as excellent model systems to investigate the role of genetic changes in cancer and specific age-related problems. At the cellular level, deficiencies in RecQ family members result in increased chromosomal abnormalities due to illegitimate recombination, suggesting functions for these helicases in recombination repair or resolution of replication blockage (6–11). Accordingly, RecQ helicases preferentially bind to and unwind substrates mimicking replication and recombination intermediates (12–18). Recent biochemical and structural studies (19–22) also indicate that specific RecQ helicases, including WRN and BLM, contain multiple DNA-binding domains. Hypothetically, it would be advantageous for proteins that act on the complex three- and four-stranded DNA structures typically associated with replication and recombination to have multiple DNA-binding domains.

The predicted roles of RecQ helicases combined with their multiple DNA-binding domains suggested that these enzymes might have, in addition to their requisite unwinding capability, other recombination functions such as strand pairing and strand exchange. The experiments described below indicate that three RecQ members (WRN, BLM, and *Drosophila melanogaster* RecQ5b (dmRecQ5b)[1]) individually possess a novel strand pairing activity that functions in several structural contexts. When this strand pairing capability acts in concert with the inherent DNA unwinding activity, WRN, BLM, and dmRecQ5b can catalyze coordinated strand exchange. Furthermore, the relatively weak pairing and exchange activity of dmRecQ5b suggests a contribution of conserved C-terminal regions in WRN and BLM to DNA binding, strand pairing, and strand exchange functions.

EXPERIMENTAL PROCEDURES

Enzymes—WRN is the only human RecQ helicase that has been demonstrated to have 3′ to 5′ exonuclease activity in addition to its requisite DNA unwinding activity (23, 24). The WRN-E84A mutant contains a glutamate to alanine substitution in the conserved nuclease domain that completely abolishes the inherent exonuclease activity of WRN, whereas its helicase activity is not affected (23, 25). Wild-type WRN and WRN-E84A proteins were individually overproduced by baculoviral infection of Sf9 insect cells and purified by a three-step chromatography procedure described previously (26), with the exception that Nonidet P-40 (0.1%) was present in all liquid chromatography buffers. BLM, *Escherichia coli* UvrD, and the *D. melanogaster* RecQ5 short isoform (dmRecQ5b) were purified as described previously (27–29). Hepatitis C virus helicase NS3 (a kind gift from Dr. S. S. Patel, Rutgers University) was purified as described previously (30). To generate the respective mock protein preparations for comparison with WRN-E84A and BLM preparations (see Fig. 2*C*), lysates either from insect cells infected with baculovirus without WRN sequences or from yeast cells transfected with vector without BLM sequences were subjected to identical purification procedures as lysates containing overexpressed WRN-E84A or BLM. The eluted fractions from the final chromatography step of each of these mock purifications were used in standard strand pairing assays to control for possible activities of proteins that potentially co-purify with WRN or BLM. Protein concentrations were determined by comparison with standards of known concentration using the Bradford assay and/or SDS-PAGE.

DNA Substrates—Oligonucleotides were obtained commercially from

* This work was supported by grants from the Ellison Medical Foundation and the University of Kentucky Research Foundation (to D. K. O.) and by NCI Grant R01 CA113371-01 from the National Institutes of Health (to D. K. O.). The costs of publication of this article were defrayed in part by the payment of page charges. This article must therefore be hereby marked "*advertisement*" in accordance with 18 U.S.C. Section 1734 solely to indicate this fact.

‖ To whom correspondence should be addressed: Graduate Center for Toxicology, 356 Health Sciences Research Bldg., University of Kentucky, 800 Rose St., Lexington, KY 40536-0305. Tel.: 859-323-3612; Fax: 859-323-1059; E-mail: dkorre2@uky.edu.

[1] The abbreviations used are: dmRecQ5b, *D. melanogaster* RecQ5b; ATPγS, adenosine 5′-*O*-(thiotriphosphate); nt, nucleotide(s); SF, superfamily; RQC, RecQ conserved; HRDC, helicase and RNase D conserved.

This is an Open Access article under the CC BY license.

Integrated DNA Technologies (Coralville, IA). Oligonucleotide sequences are given in Table I. Using standard procedures, the C80 oligomer was radiolabeled at its 5′-end with [γ-^{32}P]ATP and 3′-phosphatase-free polynucleotide kinase (Roche Applied Science). To make the fork, bubble, 80-bp blunt-ended duplex, and 24-bp partial duplex substrates, labeled C80 was annealed with 2-fold excess amounts of G80fork26, G80bub21, G80, and G24, respectively. After nondenaturing 12% PAGE to separate labeled DNA duplex products from unannealed oligonucleotides and unincorporated nucleotides, the annealed substrates and labeled single-stranded C80 were excised and purified using a Qiagen gel extraction kit. The substrates were stored at 4 °C prior to use.

Strand Pairing Assay—In the standard strand pairing assay, labeled C80 (2–125 pM) was added to reaction buffer (20-μl final volume) containing 40 mM Tris-HCl (pH 8.0), 4 mM $MgCl_2$, 0.1 mg/ml bovine serum albumin, and 5 mM dithiothreitol. Where indicated, ATP or ATPγS (1 mM) was also added. In specific experiments, NaCl (0–150 mM) was also added, or $MgCl_2$ was titrated between 0 and 40 mM or replaced with $MnCl_2$, $CaCl_2$, or $ZnCl_2$ (4 mM). Subsequently, WRN-E84A, BLM, dmRecQ5b, UvrD, NS3, or a mock preparation was added at the concentrations specified in the figure legends. Reactions were initiated by addition of unlabeled G80 (2–125 pM), followed immediately by incubation at 37 °C for 0–15 min. Protein-independent annealing was measured in identical buffers at 37 °C over much longer intervals (0–1440 min). In standard strand pairing assays, reactions were stopped by adding 0.166 volume of helicase dyes (30% glycerol, 50 mM EDTA, 0.9% SDS, 0.25% bromphenol blue, and 0.25% xylene cyanol) including excess unlabeled C80 (100 fmol) to prevent further annealing to labeled C80. Strand pairing to generate a three-way junction substrate was performed similarly, except using labeled fork substrate (12.5 pM) with WRN-E84A and G80bub21 (12.5–50 pM) in buffer minus ATP; these reactions were terminated with helicase dyes alone. DNA products were separated by nondenaturing 8% PAGE at room temperature in 1× Tris borate/EDTA. Gels were vacuum-dried and then visualized and quantitated using a Storm 860 PhosphorImager equipped with ImageQuant software (Amersham Biosciences). The percentage of duplex formed was calculated as the amount of labeled duplex DNA (C80/G80) produced divided by the total amount of labeled DNA (labeled single-stranded C80 and labeled duplex) for each lane. Similarly, the percentage of three-way intermediate (C80/G26fork/G80bub21) formed was determined with respect to the total amount of the labeled DNA species in the reaction. The amount of protein-dependent duplex formation includes subtraction of the amount of protein-independent annealing under identical conditions.

Exchange and Helicase Assays—For the exchange assays, labeled fork substrate C80/G80fork26 (12.5 pM) was incubated with or without WRN-E84A, BLM, dmRecQ5b, UvrD, or NS3 (at the concentrations indicated in figure legends) and either G80 or G80bub21 (12.5–50 pM) for 0–15 min at 37 °C in 20 μl of reaction buffer plus ATP or ATPγS (1 mM) as indicated. To estimate the maximal amount of possible protein-independent annealing that might follow putative unwinding, labeled fork substrate and G80 were heat-denatured and quick-cooled and then incubated at 37 °C for 15 min. Helicase assays were similar to exchange assays, except that labeled fork C80/G80fork26 or partial duplex C80/G24 substrate (12.5 pM each) was incubated for 15 min at 37 °C with enzyme in reaction buffer including ATP (1 mM) without addition of a third oligomer. Reactions were terminated, and DNA products were analyzed as described for the standard strand pairing assay along with duplex, bubble, and single-stranded (heat-denatured) substrate markers as indicated.

Immunodepletion of WRN-E84A and BLM—Protein G Plus/protein A-agarose bead suspensions (30 μl; Calbiochem) were equilibrated with reaction buffer and incubated with 0.5 μg of either normal rabbit IgG (Upstate Biotechnology, Inc.) or rabbit anti-WRN antibody (Novus Biologicals) for 1 h at 4 °C. After washing away unbound antibody with reaction buffer, aliquots (35 μl) of reaction buffer containing WRN-E84A (12 nM) were incubated in parallel with normal IgG-treated or anti-WRN antibody-treated beads for 10 min at 4 °C. The beads were collected by centrifugation, and the supernatants were transferred to fresh batches of IgG-treated or anti-WRN antibody-treated beads for a second immunodepletion step for 10 min at 4 °C. The beads were again collected, and the supernatants were transferred to fresh tubes. Half of each supernatant was used in a standard strand pairing assay performed for 15 min at 37 °C with labeled oligomer and its unlabeled complementary partner (12.5 pM each). The remaining half of each supernatant was subjected to SDS-PAGE and Western blotting with anti-WRN monoclonal antibody (BD Biosciences) along with an identical amount of WRN-E84A not exposed to the beads. To confirm specific immunoprecipitation of WRN, protein immobilized on the beads was liberated by boiling in SDS and analyzed in parallel with the supernatants. BLM was immunodepleted by the same method using goat anti-BLM antibody (Santa Cruz Biotechnology, Inc.).

Electrophoretic Mobility Shift Assay—Reactions containing labeled single-stranded C80 oligomer (50 pM) and wild-type WRN (0.35–2.8 nM), BLM (0.5–4 nM), or dmRecQ5b (1–72 nM) were incubated for 15 min at 4 °C in 20 μl of agarose shift buffer (20 mM glycine-KOH (pH 9.0), 1 mM ATP, 2.5 μg/ml bovine serum albumin, 4% glycerol, 0.1% Nonidet P-40, and 10 mM dithiothreitol). After adding 4 μl of native loading dye (0.25% bromphenol blue in 30% glycerol), reactions were loaded onto horizontal slab gels (0.8% agarose in 0.1× Tris borate/EDTA) that were run at 150 V for 80 min at 4 °C. After drying, free DNA and DNA-protein complexes were visualized by phosphorimaging. The percentage of DNA bound was calculated by measuring the decrease in free DNA species with increasing concentrations of WRN-E84A, BLM, and dmRecQ5b.

RESULTS

Specific RecQ Helicases Facilitate Strand Pairing—To test the hypothesis that RecQ helicases might have additional functions in recombination, oligonucleotide-based assays were developed to assess the ability of WRN, BLM, and other helicases to facilitate strand pairing and exchange. In the basic strand pairing assay (Fig. 1*A*), a radiolabeled 80-nucleotide (nt) oligomer (C80) and a fully complementary unlabeled oligomer (G80) were incubated at 37 °C with or without purified enzymes (see Table I for sequences of oligonucleotides used in this study). Because wild-type WRN has 3′ to 5′ exonuclease activity in addition to 3′ to 5′ helicase activity (23, 24), an exonuclease-deficient WRN-E84A mutant was used to prevent substrate digestion; in the presence of ATP, WRN-E84A retains DNA unwinding capability (25). Unless noted otherwise, strand pairing reactions were performed without ATP to prevent unwinding of duplex products. Protein-independent annealing of oligomers (12.5 pM each) under these conditions was minimal (6.6%) after 60 min and not complete until 24 h (Fig. 1*B*). In contrast, addition of either WRN-E84A or BLM mediated complete pairing within 10 min (Fig. 1, *B* and *C*), with the initial rate of WRN- or BLM-mediated pairing ~250-fold higher than that of protein-independent annealing. Furthermore, the extent of duplex product formation within 15 min was proportional to the WRN-E84A or BLM concentration (Fig. 1, *D* and *E*). Another RecQ helicase, dmRecQ5b, also stimulated strand pairing, but, compared with WRN-E84A and BLM, much higher protein concentrations were needed to achieve significant duplex formation (Fig. 1, *D* and *E*).

Extensive controls were performed to ensure that strand pairing activity was specific to WRN, BLM, and dmRecQ5b. All proteins used in these experiments were purified to near homogeneity (Fig. 2*A*), with recombinant dmRecQ5b, BLM, and WRN-E84A being purified after overexpression in different hosts (*E. coli*, yeast, and insect cells, respectively). Incubation of WRN, BLM, or dmRecQ5b at 70 °C prior to addition to strand pairing reactions prevented formation of duplex product (Fig. 2*B*), demonstrating that heat-labile protein factors facilitate pairing. To control for host proteins that could potentially be present at very low levels, purifications from yeast and insect cells containing vectors without BLM and WRN sequences, respectively, were performed identically to and in parallel with BLM and WRN-E84A protein purifications. In contrast to robust strand pairing activity observed for WRN-E84A and BLM, volume titrations of these "mock" preparations did not detectably increase the amounts of the duplex product above the level of protein-independent annealing (Fig. 2*C*). Furthermore, immunodepletion of WRN-E84A or BLM in solution by WRN- or BLM-specific antibody drastically reduced strand pairing activity (Fig. 2*D*) (data not shown). These experiments confirm that the observed strand pairing activities are inherent to WRN, BLM, and dmRecQ5b.

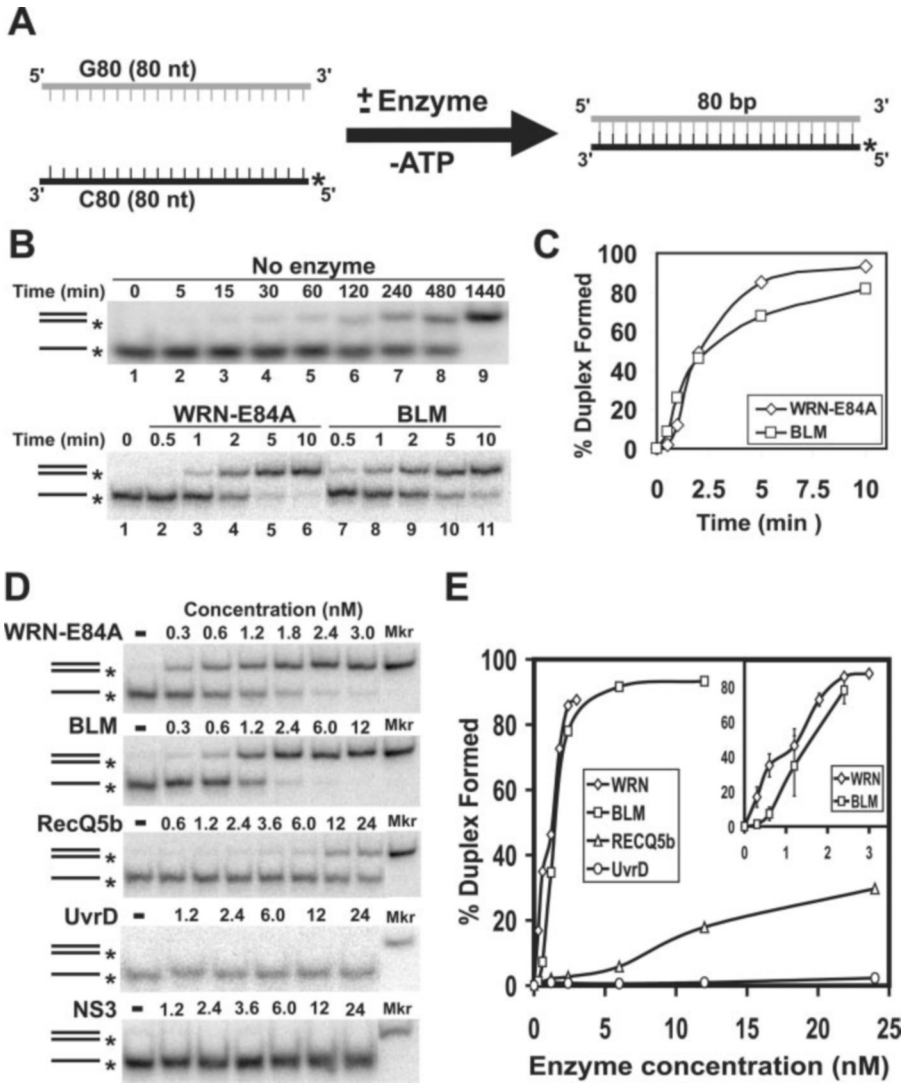

FIG. 1. **Strand pairing activities of WRN, BLM, and dmRecQ5b.** *A*, shown is a schematic diagram of the basic strand pairing assay. Radiolabeled C80 (*black*; label denoted by *asterisk*) and unlabeled complementary oligomer G80 (*gray*) are incubated in the absence or presence of protein without ATP. The strand pairing product is a labeled 80-bp blunt-ended duplex (*black-gray hybrid*). *B*, shown are the kinetics of strand pairing. As described under "Experimental Procedures," strand pairing was performed at 37 °C for the indicated times using C80 and G80 oligomers (12.5 pM each) with or without WRN-E84A (4.2 nM) or BLM (6 nM). *C*, the percentage of protein-dependent duplex product formed specifically by WRN-E84A (◇) or BLM (□) at each time point in *B*, calculated as described under "Experimental Procedures," is plotted. *D*, strand pairing reactions (as described for *B*) using WRN-E84A (0–3 nM), BLM (0–12 nM), dmRecQ5b (0–24 nM), UvrD (0–24 nM), or NS3 (0–24 nM) were incubated for 15 min. The concentrations of the enzymes used in each reaction are depicted above each lane; preformed 80-bp duplex was loaded as a marker (*Mkr*). *E*, from experiments performed as described for *D*, the amount of the protein-dependent duplex product formed at individual enzyme concentrations is plotted for WRN (◇), BLM (□), dmRecQ5b (△), and UvrD (○). Data points are the mean of three independent experiments, except for UvrD (mean of two experiments). *Inset*, data for WRN-E84A and BLM are expanded between 0 and 2.4 nM.

TABLE I
Sequences of oligonucleotides used

All sequences are depicted in 5′ to 3′ orientation. In G80fork26 and G80bub21, sequences non-complementary to C80 are underlined. For all assays, the C80 oligonucleotide was radiolabeled at the 5′-end.

Oligonucleotide	Sequence
C80	GCTGATCAACCCTACATGTGTAGGTAACCCTAACCCTAACCCTAAGGACAACCCTAGTGAAGCTTGTAACCCTAGGAGCT
G80	AGCTCCTAGGGTTACAAGCTTCACTAGGGTTGTCCTTAGGGTTAGGGTTAGGGTTACCTACACATGTAGGGTTGATCAGC
G80fork26	CTTCACAGTCAGAGTCACAGTGTGCCGGGTTGTCCTTAGGGTTAGGGTTAGGGTTACCTACACATGTAGGGTTGATCAGC
G80bub21	AGCTCCTAGGGTTACAAGCTTCACTAGGGTTGTCCAGTCACAGTCAGAGTCACAGTCCTACACATGTAGGGTTGATCAGC
G24	CCTACACATGTAGGGTTGATCAGC

Based on sequence homology, helicases are classified into five families, with most belonging to either superfamily (SF) 1 or SF2, both of which contain seven conserved sequence motifs. The RecQ helicases compose a subset of the SF2 family. To determine whether strand pairing is a general property of helicases, the well studied *E. coli* UvrD and viral NS3 enzymes, representative 3′ to 5′ helicases from SF1 and SF2, respectively, were also examined for strand pairing activity. Over a wide concentration range, neither UvrD nor NS3 (Fig. 1, *D* and *E*) facilitated significant duplex formation in the absence of ATP. Note that both UvrD and NS3 were competent for DNA unwinding in the presence of ATP (see Fig. 6, *C* and *D*). These results indicate that strand pairing activity is not present in all helicases, but is common to at least a subset of RecQ helicases.

To gain insight into the mechanism of strand pairing catalyzed by WRN, we examined the effect of the concentration of each DNA substrate (C80 and G80) on the rate of strand pairing. In these experiments, the amount of one oligomer was held constant in excess while the other was varied to generate pseudo first-order reactions (31), and the WRN-E84A-dependent formation of duplex product was measured over time. For each set of reaction conditions, the rate of pairing was then calculated during the first 5 min before the varied substrate could become limiting. The rates of each reaction at each variable substrate concentration are plotted in Fig. 3. In comparing reactions containing identical concentrations of the limiting substrate, the rates of pairing are extremely similar; for each set of reactions, the rate is also directly proportional to the concentration of the variable and limiting oligomer. Thus, our data suggest that, if the concentrations of both substrates are equimolar, the rate of the reaction would depend upon the

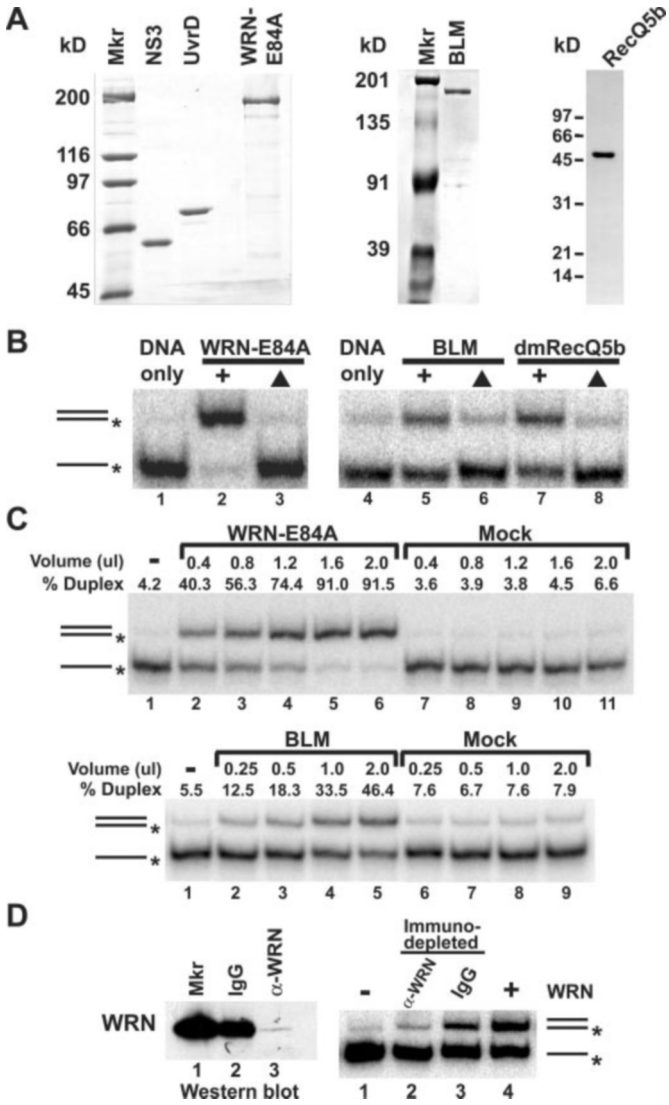

FIG. 2. **Strand pairing activity is specific to WRN, BLM, and dmRecQ5b.** *A*: shown are Coomassie Blue-stained gels of purified NS3, UvrD, and WRN-E84A (*left panel*; ~500 ng each), BLM (*middle panel*; 2 μg), and dmRecQ5b (*right panel*; 2.1 μg). It is noteworthy that the WRN-E84A, BLM, and dmRecQ5b proteins were purified to near homogeneity by different chromatography protocols from different expression systems (insect cells, yeast, and *E. coli*, respectively), eliminating the possibility of a common co-purifying contaminant. *B*: strand pairing assays using complementary oligomers (12.5 pM each) and WRN-E84A (7.2 nM), BLM (1 nM), or dmRecQ5b (12 nM) without ATP were incubated for 15 min at 37 °C and analyzed as described under "Experimental Procedures." In *lanes 3*, *6*, and *8* (▲), the proteins were heat-denatured for 10 min at 70 °C prior to performing strand pairing reactions. *C*, *upper panel*: strand pairing reactions using complementary oligomers (12.5 pM each) and WRN-E84A (0.4–2 μl, 0.6–3.0 nM) or comparable volumes of the peak fraction from a respective mock protein preparation were incubated for 15 min at 37 °C. *Lower panel*, similarly, BLM (0.25–2.0 μl, 0.4–3.2 nM) or comparable volumes of a respective mock preparation were used in strand pairing reactions containing C80 (12.5 pM) and G80 (50 pM). DNA products were analyzed as described for *B*. For each reaction, the amount (percentage) of conversion into the duplex product is indicated above each lane. *D*: solutions containing WRN-E84A (12.5 nM) were immunodepleted as described under "Experimental Procedures" using either rabbit anti-WRN IgG (*α-WRN*) or control rabbit (*IgG*) antibody immobilized on protein A/protein G Plus-agarose beads. After collection of the beads, the supernatants were split. *Right panel*, half of each immunodepleted supernatant (*lanes 2* and *3*) was incubated for 5 min with a radiolabeled 77-nt oligomer plus a complementary 71-mer (12.5 pM each); in parallel, strand pairing reactions were also performed without (*lane 1*) and with WRN-E84A (*lane 4*) not exposed to beads. DNA products were analyzed as described for *B*. *Left panel*, the other half of each supernatant was analyzed by Western blotting along with the same amount of WRN-E84A not exposed to beads (marker (*Mkr*)) (*lane 1*). The dramatic duplex product reduction in reactions in which WRN was depleted by a specific anti-WRN antibody indicates that strand pairing activity is inherent in WRN. Specific immunodepletion of BLM similarly reduced strand pairing activity (data not shown).

concentration of each, indicating that the WRN-mediated strand pairing reaction is second-order overall.

The pairing of complementary oligomers by WRN, BLM, and dmRecQ5b occurs readily in the absence of ATP. Because these helicases utilize ATP hydrolysis to drive DNA unwinding, inclusion of ATP was expected to prevent or disrupt duplex formation. Surprisingly, either WRN-E84A or BLM efficiently mediated duplex formation from these 80-mers even in the presence of ATP (Fig. 4*A*), suggesting that intermediates or products formed during pairing are not easily unwound by these helicases. However, the slightly slower rate of duplex formation by WRN-E84A and BLM in the presence of ATP than in its absence suggests a modest contribution of ATP hydrolysis and helicase activity to reversing the pairing reaction. Interestingly, addition of very poorly hydrolyzable ATPγS dramatically slowed both WRN-E84A- and BLM-dependent strand pairing (Fig. 4*A*). These results suggest that ATP-bound conformations of WRN and BLM cannot optimally complete the strand pairing reaction. Although strand pairing activity does not require ATP hydrolysis, our observation that ATPγS inhibits pairing confirms that a nucleotide-binding protein (in this case, WRN-E84A or BLM) mediates this process.

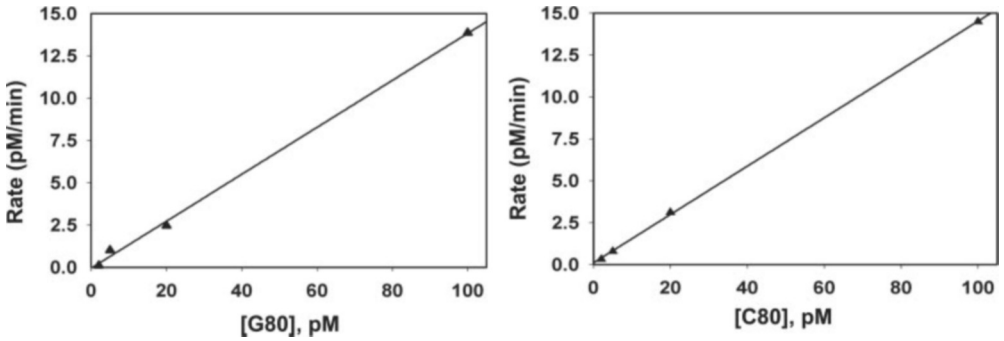

FIG. 3. **Dependence of the rate of WRN-dependent strand pairing on the concentration of each DNA substrate.** As described under "Experimental Procedures," strand pairing reactions with WRN-E84A were performed in the absence of ATP. In one series of reactions (*left panel*), the labeled C80 oligomer concentration was fixed (125 pM) while the unlabeled complementary G80 oligomer concentration was varied (2, 5, 20, or 100 pM); in another series of reactions (*right panel*), the unlabeled complementary G80 oligomer concentration was fixed (125 pM) while the labeled C80 oligomer concentration was varied (2, 5, 20, or 100 pM). For each reaction condition, time points were taken between 0 and 5 min, and the rate of each reaction was calculated using linear regression. The rate of the reaction at each concentration of the variable substrate is plotted, determining the best line through the individual data points again using linear regression. A direct dependence of the reaction rate on the concentration of each DNA substrate, as observed here, is indicative of a second-order reaction.

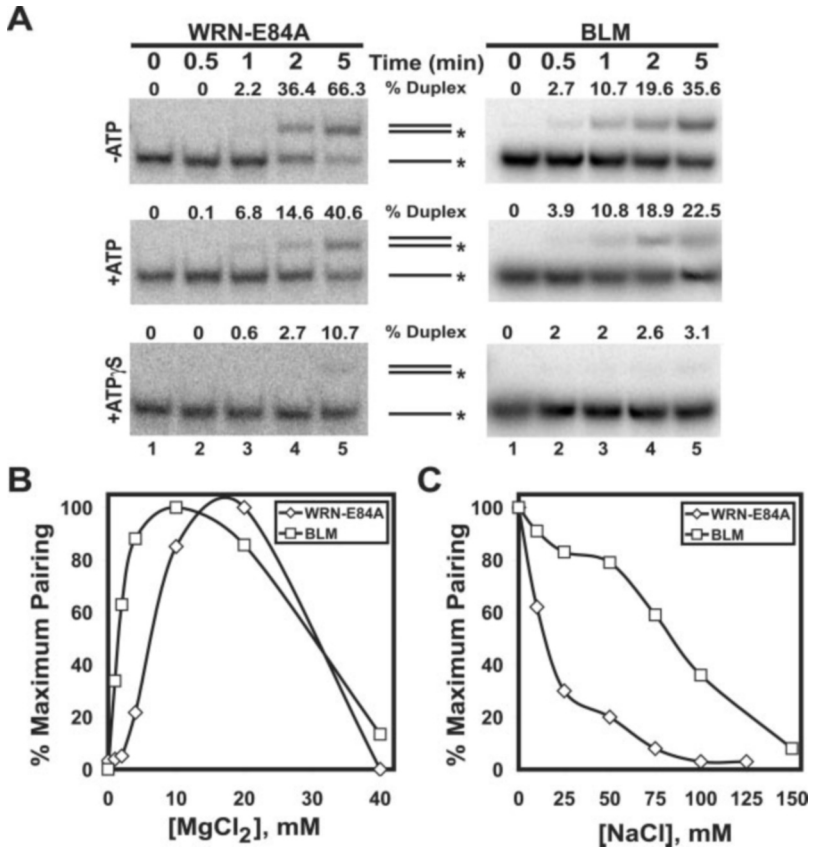

FIG. 4. **Effects of nucleotide cofactors, divalent cations, and NaCl concentration on WRN- and BLM-mediated strand pairing.** *A*, standard strand pairing assays were performed as in described under "Experimental Procedures" for the specified times with WRN-E84A (4.2 nM; *left panels*) or BLM (3 nM; *right panels*) in buffer without ATP (*upper panels*), with 1 mM ATP (*middle panels*), or with 1 mM ATPγS (*lower panes*). For each reaction, the percentage of protein-dependent duplex product formation is indicated above each lane. *B*, standard strand pairing assays were performed with WRN-E84A (3.8 nM) or BLM (7.8 nM) for 15 min as described for *A*, except that the reactions contained ATP (1 mM) and variable amounts of $MgCl_2$ (0–40 mM). After determining the amount of BLM- and WRN-E84A-dependent duplex formation at each individual $MgCl_2$ concentration, the maximal amount of pairing measured for each enzyme was set equal to 100%, and the pairing in reactions at other $MgCl_2$ concentrations was normalized to these values. The percentage of the maximal value observed for WRN-E84A (◇)- or BLM (□)-containing reactions is plotted with respect to $MgCl_2$ concentration. *C*, standard strand pairing assays were performed with WRN-E84A (4.5 nM) or BLM (10 nM) as described for *B*, except that a fixed $MgCl_2$ concentration (4 mM) and varying amounts of NaCl (0–150 mM) were used. Protein-dependent pairing for both WRN-E84A and BLM was optimal without added NaCl (0 mM). Thus, the amount of pairing measured without NaCl for each enzyme was set equal to 100%, and, similar to *B*, other reactions were normalized to these values and are plotted for WRN-E84A (◇) and BLM (□) *versus* NaCl concentration.

We also tested the effect of divalent cations and NaCl concentration on WRN-E84A- and BLM-mediated strand pairing activity. In the absence or presence of ATP, divalent cations were absolutely required for both WRN-E84A- and BLM-mediated pairing. The presence of Mg^{2+}, Mn^{2+}, or Ca^{2+} permitted WRN-E84A- and BLM-mediated pairing to varying extents, whereas Zn^{2+} did not (data not shown). In standard pairing reactions containing 1 mM ATP, the strand pairing activities of WRN-E84A and BLM were low at 1 mM $MgCl_2$, optimal between 4 and 20 mM, and dramatically inhibited at even higher

concentrations (Fig. 4*B*). These results suggest that a molar excess of Mg^{2+} over ATP enhances the strand pairing activities of both WRN-E84A and BLM. In reactions (in the presence of ATP with 4 mM $MgCl_2$) in which the effect of NaCl concentration was examined, the strand pairing activities of WRN-E84A and BLM decreased with increasing NaCl concentration (Fig. 4*C*). However, WRN-mediated strand pairing appeared to be significantly more sensitive to NaCl concentration than BLM-mediated strand pairing. Although WRN-E84A and BLM strand pairing activities might be similar at particular divalent cation and NaCl concentrations, their somewhat disparate responses to changes in conditions highlight subtle differences between these two proteins.

Because RecQ helicases most likely act on recombination or replication intermediates, we wanted to determine whether WRN or BLM facilitates strand pairing in more complex structural contexts. To this end, a fork substrate containing a 54-bp region with 26-nt single-stranded 5′- and 3′-tails was constructed from labeled C80 and a partially complementary oligomer (G80fork26) (Fig. 5*A*, *far left*). Assays with this fork substrate in combination with a third unlabeled 80-nt oligomer were performed with either WRN-E84A or BLM, again minus ATP to prevent DNA unwinding. In initial studies, this third oligomer (G80bub21) was complementary to both ends of C80, but contained a central non-complementary stretch (21 nt). Theoretically, the 5′-end of G80bub21 can pair with the 3′-tail of C80 in the fork substrate to form a three-way junction structure (Fig. 5*A*). This structure is stabilized by the non-complementary region of G80bub21 that prevents spontaneous branch migration beyond the point of complementarity. When equimolar amounts of this fork substrate and G80bub21 were incubated with WRN-E84A (Fig. 5*B*, *lanes 2–7*), a slower migrating product corresponding to the three-way junction structure was detected at 2 min and increased gradually over time, resulting in 19% of the fork being converted into the three-way junction structure by 15 min (*lane 7*). BLM acted in a similar manner, converting 38.5% of the fork substrate into the three-way junction structure after 15 min (Fig. 5*B*, *lanes 9–14*). Under these conditions, protein-independent formation of this product was not detected during this time interval (Fig. 5*B*, *lanes 1* and *8*). Although the rate of formation of this structure was slower than for the 80-bp duplex (compare Figs. 1*B* and 5*B*), either WRN-E84A or BLM dramatically stimulated strand pairing in this context. This slower rate may be due to the shorter region of complementary single-stranded DNA (26–35 bp) available to initiate pairing or to an inhibitory effect of WRN-E84A or BLM binding at the fork junction. Notably, WRN-E84A could also facilitate pairing of complementary third strands both to the unpaired region in a bubble substrate and to an unpaired single-stranded loop in a specially constructed plasmid (data not shown). Thus, WRN and BLM mediate strand pairing in multiple contexts, including multi-stranded, recombination-like structures.

WRN and BLM Catalyze Strand Exchange—ATP was withheld from the specific assays described above to assess pairing without interference from WRN or BLM unwinding. However, the formation of three-way junctions suggested that, with ATP present, these proteins might catalyze coordinated pairing and unwinding, resulting in strand exchange. Using partially complementary G80bub21 as the third strand, combined pairing and unwinding reactions would generate a labeled blunt-ended duplex containing a 21-nt bubble (Fig. 5*A*). For these experiments, the fork substrate and partially complementary G80bub21 were incubated with WRN-E84A or BLM in the absence of ATP to preform the three-way junction structure before subsequent addition of ATP. However, in these reactions, 4-fold higher concentrations of G80bub21 were used, an adjustment that markedly enhanced WRN-E84A- and BLM-mediated formation of the three-way junction during a 5-min incubation before addition of ATP (Fig. 5, compare *C* and *D*, *left panels*, *lanes 6*; with *B*, *lanes 5* and *12*); no other new products were detected. Notably, protein-independent formation of this structure was minimal even with this higher DNA concentration during the entire time course of the experiment (Fig. 5, *C* and *D*, *left panels*, *lanes 1–5*). After formation of the three-way junction in the absence of ATP by WRN-E84A (Fig. 5*C*, *left panel*) or BLM (Fig. 5*D*, *left panel*) for this 5-min interval, ATP was added, and DNA products were subsequently monitored over time. The amounts of each DNA species at individual time points were quantitated and are depicted in the bar graphs in Fig. 5 (*C* and *D*, *right panels*). One minute after ATP addition to reactions containing either WRN-E84A or BLM, the amount of the three-way junction structure decreased along with the concomitant appearance of the bubble-containing duplex (Fig. 5, *C* and *D*, *left panels*, *lanes 7*). There was also partial reversion of the three-way junction to the original fork substrate, as evidenced by an increased amount of this band at 1 min. However, the amounts of the fork substrate and three-way junction structure decreased thereafter with accompanying increases in the bubble product (Fig. 5, *C* and *D*, *right panels*). Most important, there was little or no appearance of single-stranded C80 throughout the entire time course. Taken together, these results indicate that formation of the bubble product proceeds through the three-way junction intermediate and not by complete unwinding of either the fork or the three-way junction followed by strand pairing. Thus, either WRN or BLM can catalyze a sequentially ordered strand exchange reaction by combining its strand pairing and unwinding activities.

Experiments were then performed in which the third strand (G80) was completely complementary to the labeled C80 strand of the fork substrate; here, combined pairing and unwinding yielded a labeled 80-bp blunt-ended duplex (Fig. 6*A*). In these experiments, three-way junction intermediates might spontaneously branch-migrate to yield a duplex product, thus circumventing the requirements for the ATPase and helicase activities of WRN or BLM. Thus, the effects of nucleotide cofactors on this type of exchange reaction were examined in parallel with normal unwinding reactions (without G80). In reactions without the G80 third strand (*i.e.* helicase assays), WRN-E84A or BLM unwound the fork substrate to its single-stranded components in an ATP-dependent manner (Fig. 6*B*, *lanes 2* and *8*). In contrast, in reactions containing ATP and equimolar amounts of G80, the predominant product generated by BLM or WRN-E84A was the blunt-ended duplex, whereas the amount of the single-stranded species was no higher than in the fork substrate preparation alone (Fig. 6*B*, *lanes 4* and *10*). Three-way junction intermediates were not detected in reactions using this fully complementary third strand. Remarkably, both WRN-E84A and BLM mediated almost complete conversion of the fork into the duplex within 5 min. When exchange reactions with G80 and either WRN-E84A or BLM were performed without ATP, significantly lower levels of duplex product were formed (Fig. 6*B*, *lanes 6* and *12*). With ATPγS, the duplex product levels were detectable but reduced dramatically compared with reactions with or without ATP (Fig. 6*B*, *lanes 5* and *11*). These results demonstrate that WRN and BLM readily mediate strand exchange. Generation of duplex product in the absence of ATP indicates that exchange can occur simply by the strand pairing activity of WRN or BLM followed by spontaneous branch migration. This is consistent with the lack of a three-way junction product that would be unstable due to branch migration during the reaction and

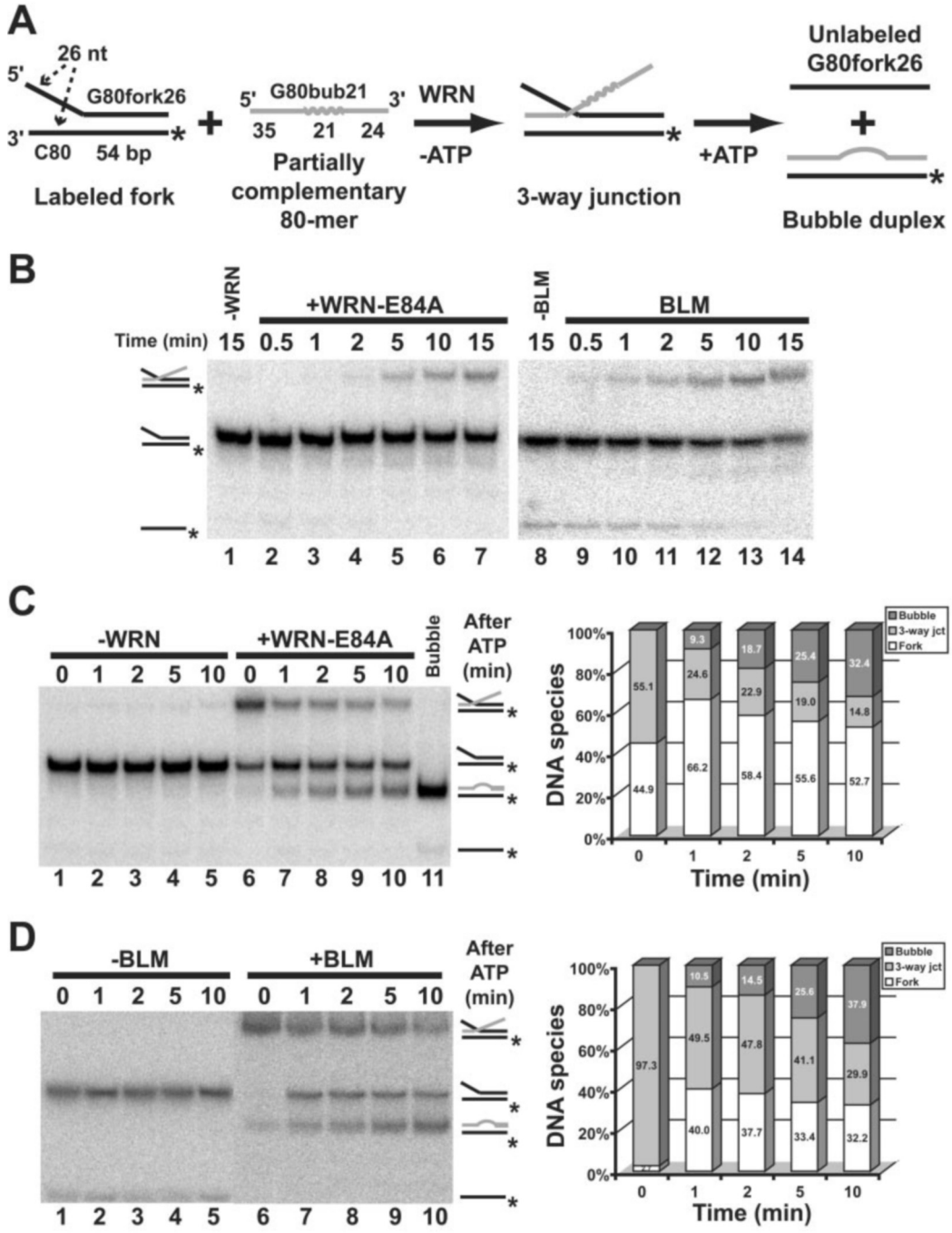

FIG. 5. **WRN-catalyzed strand exchange proceeds through three-way junction intermediates.** *A*: shown is a schematic diagram of the steps in WRN-catalyzed strand pairing and exchange reactions between a labeled fork substrate and a partially complementary 80-mer. Strand pairing in the absence of ATP generates a three-way junction intermediate that is converted to a labeled bubble substrate (plus an unlabeled oligomer) by subsequent unwinding in the presence of ATP. The positions of radiolabels are indicated by *asterisks*. *B*: in the absence of ATP, a partially complementary 80-nt oligomer (12.5 pM) without (*lanes 1* and *8*) or with WRN-E84A (3 nM; *lanes 2–7*) or BLM (6.2 nM; *lanes 9–14*) was added to the radiolabeled fork substrate (12.5 pM) and incubated at 37 °C for the indicated times. *C* and *D*: *left panels*, to preform a three-strand intermediate as described for *A*, a partially complementary oligomer (50 pM) with WRN-E84A (9 nM) or BLM (4.7 nM), respectively, was first incubated with the labeled fork substrate (12.5 pM) in the absence of ATP for 5 min at 37 °C. ATP (1 mM) was then added with continuing incubation at 37 °C for the indicated times (*lanes 6–10*). Control reactions were performed similarly, except without WRN-E84A or BLM (*lanes 1–5*). *Right panels*, the percentages of the original fork substrate, three-way junction intermediate (*3-way jct*), and bubble product measured in the WRN-E84A- and BLM-containing reactions at each individual time point after ATP addition are depicted in bar graphs. In *B–D*, DNA products were analyzed and quantitated as described under "Experimental Procedures."

subsequent gel electrophoresis. Branch migration of potential three-way junction intermediates without ATP hydrolysis also indicates that the inhibitory effect of ATPγS here is primarily on strand pairing, in agreement with earlier results (Fig. 4*A*). However, our finding that ATP enhances duplex formation strongly suggests that WRN and BLM helicase activities significantly increase the rate of the exchange by promoting branch migration. This seems particularly clear considering that, in reactions containing ATP, strand pairing is somewhat slower (Fig. 4*A*) and that some reversal of three-way junction intermediates probably occurs (as observed with exchange reactions performed with G80bub21 in Fig. 5, *C* and *D*).

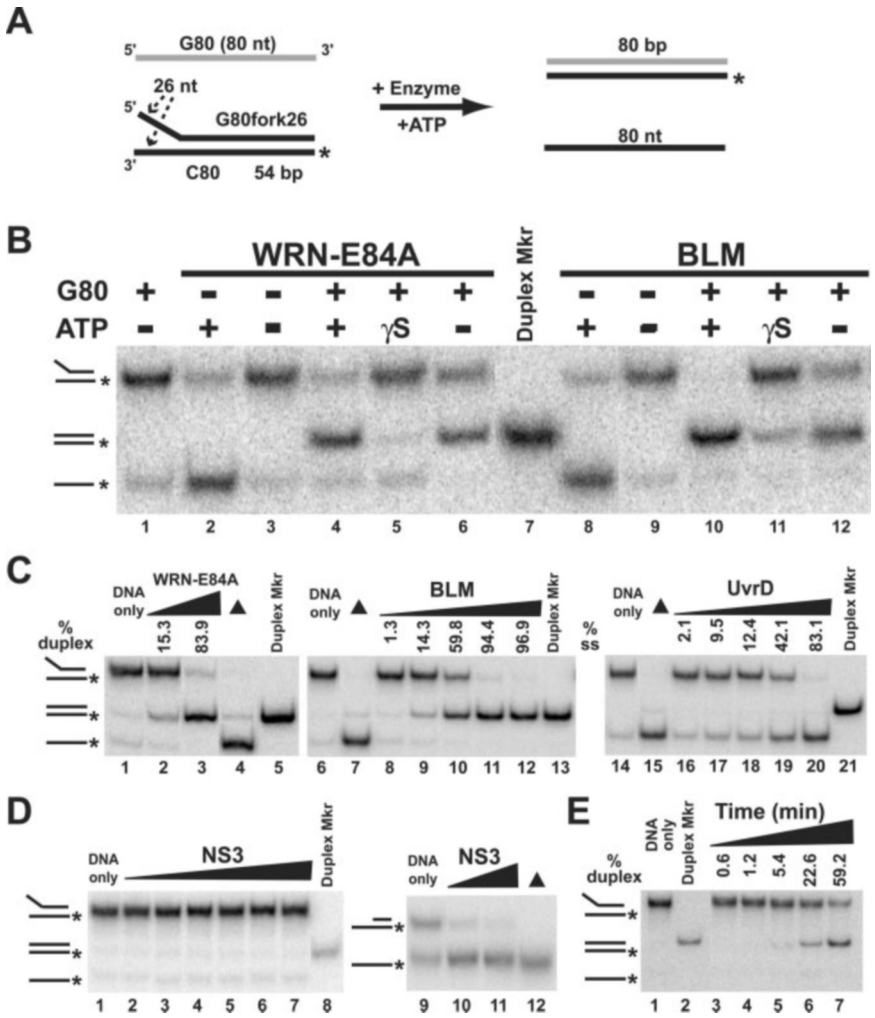

FIG. 6. **Strand exchange catalyzed by WRN and BLM.** *A*, shown is a schematic diagram of the strand exchange reactions between a labeled fork substrate and a fully complementary 80-mer. The products are a labeled 80-bp blunt-ended duplex and an unlabeled 80-nt oligomer. The positions of radiolabels are indicated by *asterisks*. *B*, the labeled fork substrate (12.5 pM) with or without fully complementary G80 (12.5 pM) was incubated with WRN-E84A (2.1 nM; *lanes 2–6*) or BLM (6 nM; *lanes 8–12*) in the absence or presence 1 mM ATP or ATPγS (γS) as indicated for 5 min at 37 °C. *C*, strand exchange reactions (as described for *B*) with ATP and WRN-E84A (1 and 3 nM; *lanes 2* and *3*), BLM (0.6–12 nM; *lanes 8–12*), or UvrD (1.2–60 nM; *lanes 16–20*) were incubated at 37 °C for 15 min. In *lanes 4*, *7*, and *15* (▲), reactions containing both the labeled fork and unlabeled 80-mer were heat-denatured, quick-cooled, and then incubated for 15 min at 37 °C. *D*, strand exchange reactions were performed as described for *C* with NS3 (1.2–36 nM; *lanes 2–7*); no exchange or unwinding was observed. However, in a standard helicase assay, incubation of NS3 (24 and 36 nM; *lanes 10* and *11*) with the 24-bp partial duplex substrate C80/G24 for 15 min resulted in production of a single-stranded product, *i.e.* unwinding. *Lane 12* (▲) contains heat-denatured C80/G24. *E*, the labeled fork substrate (12.5 pM), complementary G80 (50 pM), and WRN-E84A (9 nM) were preincubated for 5 min at 4 °C with ATP and then incubated at 37 °C for 0, 0.5, 1, 2, and 5 min (*lanes 3–7*). In *B–E*, DNA products were analyzed as described under "Experimental Procedures." The labeled 80-bp blunt-ended duplex was a marker for the strand exchange product (*Duplex Mkr*), and lanes labeled *DNA only* contain the fork substrate and G80 without protein incubated for 5 min (*E*) or 15 min (*C* and *D*) at 37 °C. In *C* and *E*, for each enzyme-containing reaction, the amount (expressed as the percentage of total labeled DNA) of protein-dependent conversion of the fork substrate to either a duplex (exchange) product for WRN-E84A and BLM or a single-stranded (*ss*; unwound) product for UvrD is indicated above each lane.

The specificity of this exchange reaction for RecQ helicases and its dependence on protein concentration were also examined. Experiments with approximately equimolar amounts of the fork substrate and fully complementary G80 were performed with ATP and increasing amounts of WRN-E84A, BLM, UvrD, or NS3. WRN-E84A and BLM readily mediated the concentration-dependent formation of the duplex (strand exchange) without significant increases in single-stranded C80 (unwinding) (Fig. 6*C*). In contrast, UvrD mediated unwinding of the fork to the single-stranded product without detectable duplex formation. As a control, the fork substrate was heat-denatured and then incubated with only G80 to assess potential contributions of protein-independent annealing to duplex formation. The duplex product was barely detectable under these conditions (Fig. 6*C*, *lanes 4*, *7*, and *15*). Thus, we can definitively conclude that the strand pairing activities of WRN-E84A and BLM facilitate duplex product formation in these strand exchange reactions. When NS3 was used in reactions containing the fork plus complementary G80, neither unwinding nor exchange was observed (Fig. 6*D*, *lanes 2–7*); however, NS3 was competent for unwinding of a 24-bp partial duplex substrate (*lanes 10 and 11*). In comparison with the rapid conversion of the fork into the duplex product in these reactions by WRN-E84A or BLM, the inability of UvrD or NS3 to mediate formation of duplex products suggests that strand exchange activity is specific to a subset of RecQ helicases.

The lack of single-stranded products in our exchange reactions suggested that the strand pairing and unwinding activities of WRN and BLM might be concerted. To determine whether unwinding occurs independently of or is coordinated with pairing in exchange reactions with G80, a kinetic analysis was performed (Fig. 6*E*). In this experiment, WRN-E84A was

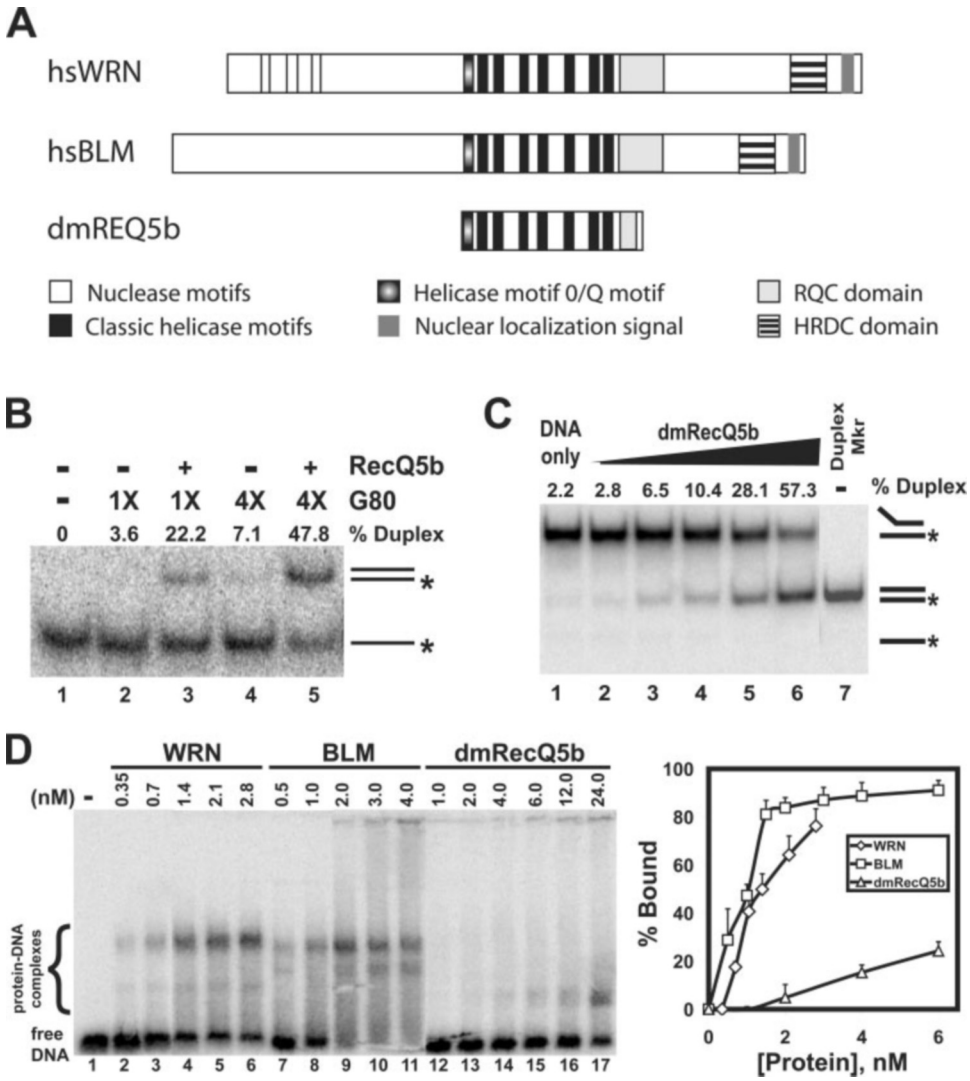

FIG. 7. **Reduced strand pairing and exchange activities in dmRecQ5b.** *A*: shown is the domain structure of RecQ homologs. *Homo sapiens* (*hs*) WRN, *H. sapiens* BLM, and the dmRecQ5b isoform are aligned with respect to their conserved helicase sequence motifs. Individual domains are depicted as shown. *B*: strand pairing reactions were performed and analyzed as described for Fig. 1*B* with dmRecQ5b (12 nM) and the G80 oligomer at either 12.5 pM (*1X*; *lanes 2* and *3*) or 50 pM (*4X*; *lanes 4* and *5*) for 15 min at 37 °C. For each reaction, the amount of the annealed duplex product (expressed as the percentage of total labeled DNA) is indicated above each lane. *C*: strand exchange reactions were performed as described for Fig. 6*C* with dmRecQ5b (2.4–60 nM; *lanes 2–6*), except the G80 oligomer concentration was 50 pM. In these reactions, the amount of the exchanged duplex product (expressed as the percentage of total labeled DNA) is indicated above each lane. The labeled 80-bp blunt-ended duplex was a marker for the strand exchange product (*Duplex Mkr*). *D*: *left panel*, in electrophoretic mobility shift assays, the indicated amounts of wild-type WRN (*lanes 2–6*), BLM (*lanes 7–11*), or dmRecQ5b (*lanes 12–17*) were incubated with a labeled single-stranded DNA oligomer (C80) and subjected to native agarose gel electrophoresis as described under "Experimental Procedures." The percentage of oligomer bound by protein was determined by reductions in the amount of free DNA compared with reactions without protein. *Right panel*, data obtained from multiple experiments, three each for WRN (◇) and BLM (□) and five for dmRecQ5b (△), are plotted for protein concentrations between 0 and 6 nM.

preincubated with both DNA components and ATP for 5 min at 4 °C before initiating the reaction at 37 °C. Notably, the duplex product was detectable by 1 min and formed efficiently within 5 min, with little or no single-stranded product detected early in the time course, suggesting that unwinding does not occur independently of pairing. Although the sequence of events in these experiments could not be determined definitively, the pairing and helicase activities of WRN and BLM apparently perform concerted strand exchange. This interpretation is also consistent with our sequentially ordered exchange reactions (Fig. 5, *C* and *D*).

Involvement of Conserved C-terminal Domains in Strand Pairing and Exchange—In an effort to identify the regions that participate in strand pairing, the amino acid sequences of WRN, BLM, and dmRecQ5b were compared. Notably, regions in WRN and BLM that are N-terminal to the helicase domain lack significant homology; dmRecQ5b contains minimal sequences N-terminal to its helicase domain. However, C-terminal to the conserved helicase motifs, some RecQ members, including WRN and BLM, contain two additional regions of homology known as the RecQ conserved (RQC) and helicase and RNase D conserved (HRDC) domains (Fig. 7*A*). Both domains have been implicated in DNA binding (19–22). Notably, dmRecQ5b contains the conserved helicase sequence motifs, but lacks the HRDC domain and the C-terminal part of the RQC domain (Fig. 7*A*). Thus, the absence of these C-terminal sequences that are postulated to participate in DNA binding might be responsible for the relatively poor strand pairing activity of dmRecQ5b compared with that of WRN or BLM (Fig. 1, *D* and *E*). To test this hypothesis, strand pairing was performed with dmRecQ5b, comparing equimolar (12.5 pM) and 4-fold higher (50 pM) levels of the unlabeled G80 oligomer. This adjustment more than doubled dmRecQ5b-dependent duplex formation (from 18.6 to 40.7%) in 15 min (Fig. 7*B*). As observed

for strand pairing, dmRecQ5b-dependent strand exchange was detectable but weak when using equimolar DNA concentrations (data not shown). Therefore, strand exchange assays were also performed with dmRecQ5b using 4-fold higher levels of the fully complementary third strand (G80). Under these conditions, dmRecQ5b readily facilitated strand exchange without detectable unwinding (Fig. 7*C*). To investigate whether the weaker strand pairing and exchange activities of dmRecQ5b are specifically due to lower DNA binding capability, electrophoretic mobility shift assays were performed to directly compare the affinities of WRN, BLM, and dmRecQ5b for an 80-nt single-stranded DNA oligomer (C80). WRN, BLM, and dmRecQ5b could all form complexes with C80 using this technique, but significantly higher dmRecQ5b concentrations were required to detect complex formation (Fig. 7*D*, *left panel*). Although some of these complexes were stable (slower mobility bands), others appeared to be disrupted during electrophoresis (note smears trailing upward from free DNA). Thus, total DNA binding affinity was determined by quantitating the reduction in free DNA signal when protein was present. The data plotted for 0–6 nM protein (Fig. 7*D*, *right panel*) clearly show that WRN and BLM have a similar binding affinity for this 80-nt oligomer, whereas the binding affinity of dmRecQ5b is much lower. Much higher concentrations of dmRecQ5b (36–72 nM) were needed to obtain almost complete binding of this oligomer. Based on the amounts of protein necessary to retard 25, 50, and 75% of the DNA substrate, we estimate that WRN and BLM have ~6–10-fold higher binding affinities compared with dmRecQ5b. Taken together, our results strongly suggest that the relatively weak strand pairing and exchange activities of dmRecQ5b are due to lower DNA binding affinity and suggest that regions C-terminal to the helicase domain (putatively the RQC and HRDC domains) contribute to these functions.

DISCUSSION

In this study, we have demonstrated that WRN, BLM, and dmRecQ5b have a novel strand pairing capability that, when coordinated with the well established helicase activity, essentially endows these RecQ helicases with a strand exchange function. In strand exchange reactions containing a fork duplex and a complementary third strand, the pairing and unwinding activities occur in a concerted manner, as no significant unwinding independent of pairing could be detected. Both the strand pairing and strand exchange activities appear to be specific to these RecQ helicases, as only unwinding was observed in other helicases tested. It is quite logical that strand pairing and exchange functions would be associated with RecQ helicases because these enzymes are postulated to act in recombination or replication restart pathways that involve swapping of DNA strands (6–10).

Strand pairing mediated by WRN is a second-order reaction, with the reaction rate demonstrated to be dependent on the concentration of both DNA substrates. Changes in reaction conditions also had significant effects on the strand pairing activities of WRN and BLM. The presence of divalent cations was required for WRN- or BLM-mediated pairing, whereas increasing concentrations of NaCl were inhibitory. WRN- or BLM-dependent pairing was optimal when free Mg^{2+} was available (in a molar excess over ATP), suggesting an effect of divalent cations on protein conformation independent of their association with ATP in the nucleotide-binding pocket of these RecQ helicases. Interestingly, our observations with WRN and BLM regarding the effects of divalent cations and NaCl on strand pairing are reminiscent of previous experiments characterizing RecA-mediated strand pairing and exchange (32). Additional experiments need to be performed to address the mechanism of strand pairing by these RecQ helicases and exactly how reaction conditions affect this process.

Surprisingly, WRN- or BLM-mediated duplex product formation was robust in the standard strand pairing assay even under conditions that permitted DNA unwinding (with ATP). Thus, at least in the context of our complementary 80-nt oligomers, strand pairing outcompetes unwinding. In standard helicase assays with simple partial duplex substrates, strand pairing and unwinding activities would also tend to counteract one another. Interestingly, previous studies of the helicase activity catalyzed by WRN or BLM alone indicate that both proteins have difficulty unwinding duplexes in the range of 50–70 bp or longer (33–35). Based on our findings, the strand pairing activities of WRN and BLM may increasingly counteract unwinding as the length of DNA duplex increases. This suggests that both WRN and BLM may actually be more robust DNA-unwinding enzymes than indicated by earlier measurements.

Despite the seeming competition between these activities on simple duplexes, our experiments clearly indicate that coordination between the strand pairing and DNA unwinding activities of WRN or BLM readily achieves strand exchange between a partial duplex and a complementary third strand. Notably, BLM and WRN have previously been shown to disrupt preformed Holliday junction substrates (12, 13), a process that involves branch migration and that requires the ATPase and helicase functions of these enzymes. Our results significantly extend these findings by demonstrating that these enzymes also have an inherent ability to form recombination structures involving three (and possibly four) DNA strands and subsequently to branch-migrate such structures. Moreover, because strand pairing necessarily occurs during branch migration, it is possible that the strand pairing and helicase activities of WRN and BLM act in concert to enhance branch migration on physiological recombination structures. Such coordination may help explain the ability of WRN and BLM to catalyze branch migration unidirectionally through long stretches of DNA (12, 13). The ability of a protein factor to combine strand pairing with DNA unwinding to catalyze a strand exchange reaction would be extremely valuable in performing certain DNA transactions during replication or recombination. Specifically, this enzymatic property could potentially regress a replication fork with pairing of nascent strands (to form a Holliday junction or so-called "chicken foot"), assist formation and branch migration of heteroduplex structures, disrupt illegitimate heteroduplexes, or resolve normal heteroduplexes with concomitant regeneration of duplex DNA. In agreement with the latter possibility, recent reports suggest that BLM (in association with topoisomerase IIIα) and WRN act to resolve recombination intermediates (9, 36).

Our experiments indicate that strand pairing and exchange activities are found within at least three RecQ family members. Interestingly, recent experiments using the long isoform of human RECQ5 (RECQ5β) suggest that this RecQ helicase also facilitates strand pairing and that sequences C-terminal to the helicase domain participate in DNA binding and strand pairing (37). The N-terminal regions of human RECQ5β and dmRecQ5b (used in our experiments) are highly homologous, but the latter is truncated downstream of the helicase domain in the middle of the RQC domain and lacks C-terminal sequences found in human RECQ5β. Our experiments show that dmRecQ5b has weaker DNA binding affinity compared with either WRN or BLM and that its strand pairing and exchange activities are stimulated by increasing DNA concentrations. Thus, we conclude that conserved C-terminal domains in specific RecQ members harbor DNA binding properties that assist strand pairing and exchange. As the HRDC domain conserved between WRN and BLM is not readily identifiable in human

RECQ5β, we postulate that an intact RQC domain participates in these DNA binding and strand pairing functions. Furthermore, our findings infer that, in some RecQ members, juxtaposition of the helicase domain with C-terminal DNA-binding domains results in a three-dimensional conformation specifically evolved to catalyze strand exchange within recombination or replication intermediates. Thus, RecQ helicases, particularly those with additional C-terminal DNA-binding domains, might constitute a family of structure-specific strand exchange enzymes. Notably, loss of critical strand exchange functions is consistent with the illegitimate recombination and cancer-prone phenotypes of human syndromes caused by RecQ helicase deficiencies.

Acknowledgments—We thank Drs. J. Campisi, M. D. Gray, J. Oshima, I. D. Hickson, V. A. Bohr, G.-M. Li, and S. S. Patel for providing experimental reagents and A. Combs for technical assistance.

REFERENCES

1. Ellis, N. A., Groden, J., Ye, T. Z., Straughen, J., Lennon, D. J., Ciocci, S., Proytcheva, M., and German, J. (1995) *Cell* **83,** 655–666
2. Yu, C.-E., Oshima, J., Fu, Y. H., Wijsman, E. M., Hisama, F., Alisch, R., Matthews, S., Nakura, J., Miki, T., Ouais, S., Martin, G. M., Mulligan, J., and Schellenberg, G. D. (1996) *Science* **272,** 258–262
3. Kitao, S., Shimamota, A., Goto, M., Miller, R. W., Smithson, W. A., Lindor, N. M., and Furuichi, Y. (1999) *Nat. Genet.* **22,** 82–84
4. Goto, M. (1997) *Mech. Ageing Dev.* **98,** 239–254
5. Oshima, J., and Martin, G. M. (2000) *Nature* **408,** 263–266
6. Shen, J.-C., and Loeb, L. A. (2000) *Trends Genet.* **16,** 213–220
7. van Brabant, A. J., Stan, R., and Ellis, N. A. (2000) *Annu. Rev. Genomics Hum. Genet.* **1,** 409–459
8. Myung, K., Datta, A., Chen, C., and Kolodner, R. D. (2001) *Nat. Genet.* **27,** 113–116
9. Satigny, Y., Makienko, K., Swanson, C., Emond, M. J., and Monnat, R. J. (2002) *Mol. Cell. Biol.* **22,** 6971–6978
10. Hickson, I. D. (2003) *Nat. Rev. Cancer* **3,** 169–178
11. Davalos, A. R., and Campisi, J. (2003) *J. Cell Biol.* **162,** 1197–1209
12. Karow, J. K., Constantinou, A., Li, J.-L., West, S. C., and Hickson, I. D. (2000) *Proc. Natl. Acad. Sci. U. S. A.* **97,** 6504–6508
13. Constantinou, A., Tarsounas, M., Karow, J. K., Brosh, R. M., Bohr, V. A., Hickson, I. D., and West, S. C. (2000) *EMBO Rep.* **1,** 80–84
14. van Brabant, A. J., Ye, T., Sanz, M., German, J. L., Ellis, N. A., and Holloman, W. K. (2000) *Biochemistry* **39,** 14617–14625
15. Shen, J.-C., and Loeb, L. A. (2000) *Nucleic Acids Res.* **28,** 3260–3268
16. Brosh, R. M., Waheed, J., and Sommers, J. A. (2002) *J. Biol. Chem.* **277,** 23236–23245
17. Orren, D. K., Theodore, S., and Machwe, A. (2002) *Biochemistry* **41,** 13483–13488
18. Ozsoy, A. Z., Ragonese, H. M., and Matson, S. W. (2003) *Nucleic Acids Res.* **31,** 1554–1564
19. Morozov, V., Mushegian, A. R., Koonin, E. V., and Bork, P. (1997) *Trends Biochem. Sci.* **22,** 417–418
20. Liu, Z., Macias, M. J., Bottomley, M. J., Stier, G., Linge, J. P., Nilges, M., Bork, P., and Sattler, M. (1999) *Struct. Fold Des.* **7,** 1557–1566
21. Bernstein, D. A., Zittel, M. C., and Keck, J. L. (2003) *EMBO J.* **22,** 4910–4921
22. von Kobbe, C., Thoma, N. H., Czyzewski, B. K., Pavletich, N. P., and Bohr, V. A. (2003) *J. Biol. Chem.* **278,** 52997–53006
23. Huang, S., Li, B., Gray, M. D., Oshima, J., Mian, I. S., and Campisi, J. (1998) *Nat. Genet.* **20,** 114–116
24. Shen, J.-C., Gray, M. D., Oshima, J., Kamath-Loeb, A. S., Fry, M., and Loeb, L. A. (1998) *J. Biol. Chem.* **273,** 34139–34144
25. Machwe, A., Xiao, L., Theodore, S., and Orren, D. K. (2002) *J. Biol. Chem.* **277,** 4492–4504
26. Orren, D. K., Brosh, R. M., Nehlin, J. O., Machwe, A., Gray, M. D., and Bohr, V. A. (1999) *Nucleic Acids Res.* **27,** 3557–3566
27. Mechanic, L. E., Hall, M. C., and Matson, S. W. (1999) *J. Biol. Chem.* **274,** 12488–12498
28. Ozsoy, A. Z., Sekelsky, J. J., and Matson, S. W. (2001) *Nucleic Acids Res.* **29,** 2986–2993
29. Karow, J. K., Chakraverty, R. K., and Hickson, I. D. (1997) *J. Biol. Chem.* **272,** 30611–30614
30. Levin, M. K., and Patel, S. S. (1999) *J. Biol. Chem.* **274,** 31839–31846
31. Jencks, W. P. (1969) *Catalysis in Chemistry and Enzymology*, McGraw-Hill Inc., New York
32. Cox, M. M., and Lehman, I. R. (1982) *J. Biol. Chem.* **257,** 8523–8532
33. Shen, J.-C., Gray, M. D., Oshima, J., and Loeb, L. A. (1998) *Nucleic Acids Res.* **26,** 2879–2885
34. Brosh, R. M., Orren, D. K., Nehlin, J. O., Ravn, P. H., Kenny, M. K., Machwe, A., and Bohr, V. A. (1999) *J. Biol. Chem.* **274,** 18341–18350
35. Brosh, R. M., Li, J.-L., Kenny, M. K., Karow, J. K., Cooper, M. P., Kureekattil, R., Hickson, I. D., and Bohr, V. A. (2000) *J. Biol. Chem.* **275,** 23500–23508
36. Wu, L., and Hickson, I. D. (2003) *Nature* **426,** 870–874
37. Garcia, P. L., Liu, Y., Jiricny, J., West, S. C., and Janscak, P. (2004) *EMBO J.* **23,** 2882–2891